THE JOURNAL OF BIOLOGICAL CHEMISTRY
Vol. 268, No. 24, Issue of August 25, pp. 18119-18127, 1993
Printed in U.S.A.

Nonenzymatic Glycation Alters Protein Structure and Stability

A STUDY OF TWO EYE LENS CRYSTALLINS*

(Received for publication, April 6, 1993)

Manni Luthra‡ and Dorairajan Balasubramanian§

From the Center for Cellular and Molecular Biology, Uppal Road, Hyderabad 500 007, India

We have investigated the effect of nonenzymatic glycation (fructation) *in vitro* on the structure and stability of two proteins that are glycated *in vivo* as a consequence of high endogenous levels of sugar. We find that whereas fructation leads to the structural destabilization of the monomeric γ-crystallin from the core of the eye lens, it leads to an increase in stability in the multimeric α-crystallin of the lens cortex. Thus, while glycated γ-crystallin shows (*a*) a longer wavelength of fluorescent emission, indicating a greater exposure of its aromatic side chains to the medium; (*b*) a reduced secondary structural content; and (*c*) a more facile denaturation by thermodynamic and chemical means, α-crystallin displays the opposite behavior. Furthermore, α-crystallin shows an increased tendency toward multimeric aggregation upon fructation. We interpret these differences in the broad context of the effects of neutralization of positive charges on protein structure and stability. Fructation tends to destabilize γ-crystallin, by effecting a significant reversal in the balance of charges in the protein, at physiological pH. α-Crystallin is a multimeric protein whose pI is lower than its pH of optimum stability. Fructation in this case effectively neutralizes the cationic charges and promotes conformational order. This study indicates that although glycation brings about similar changes in the covalent chemical structures of proteins, its influence on the three-dimensional structures of different proteins can be different.

Proteins are known to react nonenzymatically with sugars. This reaction, commonly termed glycation, occurs primarily through the formation of a Schiff base between the aldehyde (or keto) groups of the sugars and amino groups of the protein chain (1). The Schiff base thus generated subsequently goes through a number of reactions (Fig. 1) to yield fluorescent brown pigments called advanced glycation end products (2–6). Although very little is known about the structures of these glycation end product molecules, fluorescent products have been demonstrated to form upon the incubation of sugars with proteins in aqueous solution (7, 8) and also upon the incubation of sugars with derivatives of the amino acid lysine (9). These products have also been recently detected immunologically (9–11) in tissue extracts.

A number of biological and biochemical abnormalities associated with diabetes and aging (such as stiffening of arteries and joints (12), vascular narrowing (13), altered cell and protein turnover (14), and cataract formation (15)) have been attributed to the nonenzymatic glycation of proteins. It has been suggested that glycation leads to impaired protein digestibility (16), cross-linking (17, 18), insolubility (19), increased resistance to heat denaturation (20), and the generation of yellow and brown chromophores (18, 21).

This investigation on protein glycation stems from our interest (22–24) in processes affecting the structures and stabilities of the eye lens proteins upon aging. The lens is a tissue that does not turn over (25). Therefore, it tends to accumulate changes in its constituent proteins, termed the crystallins. The crystallins constitute ~40% of the wet weight of the lens and are primarily responsible for the maintenance of its transparent state (26). Thus, if glycation were to lead to changes in crystallin structure and stability, the normally ordered molecular arrangement of crystallins (27, 28) in lens fiber cells would be altered, leading in turn to changes in the scattering and refractive properties of the lens. In this connection, it is worth noting that (i) sugars are known to accumulate in the lens under clinical conditions (29); (ii) glycated crystallins and advanced glycation end product molecules have been identified in diabetic human lenses (5, 30); (iii) glycation has been observed to lead to inter-crystallin cross-links (31) and chromophores that absorb visible light (32); (iv) a time-dependent increase in glycation of crystallins occurs in streptozotocin-induced diabetic rats (33); and (v) an epidemiological connection between diabetes and cataracts has been established (30, 34). Current opinion holds that the etiology of cataracts in diabetic patients is related to the progressive glycation of lens crystallins.

In tissues such as the lens, where the sorbitol pathway is active, the conversion of glucose to fructose can lead to a rise in the level of fructose, making it twice as concentrated as glucose (35). It is thus more relevant to study the reaction of lens proteins with fructose. In this study, the effects of glycation by fructose, termed fructation, on the monomeric γ-crystallin and the multimeric α-crystallin have been studied. This comparison is of interest because the core (or nucleus) of the lens is rich in γ-crystallin, while the cortex is rich in α-crystallin (25). Also, while γ-crystallin is basic (the various γ-crystallin chains have isoelectric points ranging from 7.0 to 8.5) and monomeric (molecular mass of ~21 kDa), α-crystallin is a large aggregate with a molecular mass ranging from 350 to 800 kDa or even higher (36), composed of two types of acidic subunits (αA and αB) with isoelectric points below 5. Since glycation is likely to acidify a protein because of its neutralizing effect on positive charges, its effects on a protein could be expected to depend on the specific contribution made by electrostatic interactions to the stability of the protein.

We have studied the effects of fructation on the secondary, tertiary, and quaternary structures of γ- and α-crystallins. Our investigation has specifically been aimed at monitoring the effects of glycation on (i) the isoelectric points of lens crystallins, (ii) the structures of lens crystallins in aqueous solution,

* The costs of publication of this article were defrayed in part by the payment of page charges. This article must therefore be hereby marked "*advertisement*" in accordance with 18 U.S.C. Section 1734 solely to indicate this fact.

‡ Recipient of a senior research fellowship from the Council of Scientific and Industrial Research.

§ Honorary Professor of the Jawaharlal Nehru Center for Advanced Scientific Research, Bangalore, India. To whom correspondence should be addressed. Tel.: 91-842-853487, 91-842-852241; Fax: 91-842-851195; Telex: 0425-7046CCMBIN.

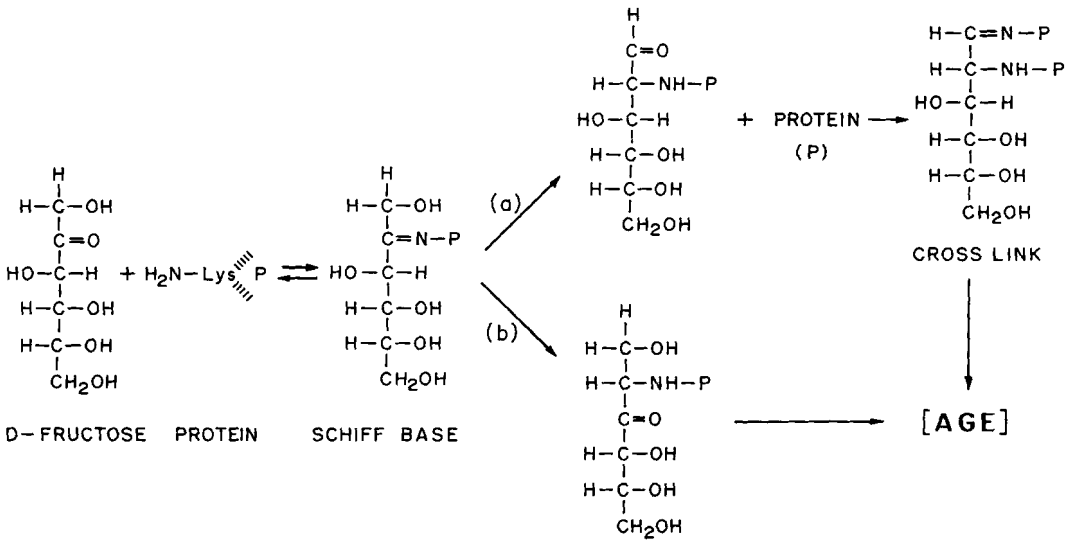

FIG. 1. **General scheme showing reaction of fructose with protein (*P*).** *AGE*, advanced glycation end products.

(iii) the self-associative behavior of subunits in the multimeric α-crystallin, and (iv) the structural stability of crystallins and their denaturation profiles. Earlier work had indicated tertiary structural alterations in α-crystallin upon glycation (37–39). Our results show that glycation has contrasting effects on the structural stabilities of the two crystallins.

MATERIALS AND METHODS

Preparation of Lens Proteins—Bovine lenses (8 to 10) were decapsulated and homogenized in 0.1 M Tris buffer, pH 7.4, containing 0.5 M NaCl, 1 mM EDTA, and 0.1% NaN_3. The insoluble protein fraction and membrane debris were removed by centrifugation at 30,000 × *g* for 30 min. The supernatant was chromatographed on a Sephacryl S-200 gel filtration column (0.04 × 1.8 m) to separate the individual crystallins. Each of the crystallins was dialyzed repeatedly against water and stored in the lyophilized form.

In Vitro Incubations—α- and γ-crystallins (6 mg/ml) were incubated with 0.5 M fructose in 0.05 M phosphate buffer, pH 7.4, containing 0.1% azide. For each of the above incubations, a corresponding control batch that did not contain fructose was also set up. To ensure sterility, the solutions were passed through sterile, disposable Falcon filter units (Becton Dickinson). The solutions were incubated in these filter units at 37 °C for over 8 weeks to ensure saturation fructation (33).

Isolation of Glycated Crystallins Using Boronate Affinity Chromatography—Chromatography was carried out on Glyc-Affin GHb columns (Isolab, Inc., Akron, OH) according to the method of Perry *et al.* (40). The incubated crystallin reaction mixture was dialyzed extensively against 0.25 M ammonium acetate buffer, pH 8.5, and placed on a Glycogel column equilibrated with the same buffer. Unbound proteins were eluted with this buffer, and the bound proteins were eluted with buffer containing 0.2 M sorbitol. (Following this, the column was regenerated with 0.1 M HCl.) Fractions measuring 1 ml in volume were collected and monitored for absorption at 280 nm. The fractions corresponding to the bound protein were pooled together, dialyzed, and concentrated.

Extent of Glycation—The amount of sugar bound to the protein was determined by measuring the amount of formaldehyde released by periodate oxidation of C-1 hydroxyls in the Amadori product form of the glycated protein (41). The method of Ahmed and Furth (42) was used for this purpose.

SDS-PAGE[1] *and Isoelectric Focusing Gel Electrophoresis*—Homogeneous 12.5% SDS-polyacrylamide gels were run on the Pharmacia LKB Biotechnology Phastsystem assembly to examine possible formation of covalently cross-linked (non-disulfide) protein aggregates. Isoelectric focusing was also done on the Phastsystem assembly using precast gels in the pI range 3–9 to determine alterations in isoelectric points upon glycation.

Calculation of Protein pI Values—The CHARGPRO subroutine in the PC/GENE software was used to compute and to plot the electric charge of various crystallin subunits as a function of pH. This computation was based on a standard set of p*K* values for the titratable amino acids, assuming complete accessibility to the solvent. (In the case of the α-crystallin subunits, the blocking of the NH_2 terminus was taken into account in the calculation.) The subroutine uses an algorithm that iterates the pH dependence of a protein's charge to deduce its isoelectric point.

High Pressure Gel Permeation Chromatography—A Pharmacia HPLC system with a model LCC 2552 controller, model 2248 single pump, Shimadzu SPD 6A UV detector, and Pharmacia model 2221 recording integrator were used to analyze glycated and unglycated proteins. Samples were chromatographed on a TSK 3000 SW column (7.5 × 600 mm) coupled with a TSK 4000 SW column (7.5 × 600 mm) protected with the TSK SWG guard precolumn (7.5 × 75 mm). Absorbance was monitored at 280 nm with isocratic flow at 0.5 ml/min. The isocratic mobile phase consisted of 50 mM sodium phosphate, 50 mM sodium chloride, pH 6.8.

Determination of Protein Concentration—Protein concentrations were determined using amino acid analysis data. Samples were hydrolyzed in evacuated sealed tubes in 6 N HCl at 110 °C for 24 h, followed by drying under vacuum. The amino acid composition of the proteins was determined with a Pharmacia Alpha Plus amino acid analyzer. Calculations were based on the assumption that each nanomole of the 173-amino acid long γ-crystallin peptide chain would yield 7 nmol of isoleucine, while each nanomole of the 174-amino acid long α-crystallin chain would yield 10 nmol of valine. A comparison of sequence data shows that the γ-crystallins II, IIIa, IIIb, and IV, all of which are 173 amino acids long, contain 7 isoleucines each, although the other amino acids differ in composition. Similarly, the two α-crystallin chains αA and αB, both of which are 174 amino acids long, contain 10 valines each.

Spectral Measurements—Absorption spectra were recorded on a Hitachi model 330 spectrophotometer. Fluorescence spectra were recorded on a Hitachi model F-4000 spectrofluorometer. For fluorescence measurements at various temperatures, a solution of water and ethylene glycol from a thermostatically controlled circulator bath was passed through the outer chamber of the fluorescence cuvette, and temperature measurements were made using the thermocouple probe of a BAT-10 thermometer (Physitemp). Circular dichroic spectra were recorded in Δ*A* units with a Jobin-Yvon Mark V Dichrograph connected to an Apple IIe computer. Mean residue ellipticity plots were obtained using the expression $[\theta] = (\Delta A_{obs} \times 3300 \times MRW)/c \times l$, where the mean residue weight (MRW) of both crystallins was taken to be 115, *c* is the concentration of protein in milligrams/milliliter obtained through amino acid analysis, and *l* is the path length of the cuvette in centimeters.

Protein Denaturation—Guanidine hydrochloride (GdnHCl) from Serva was recrystallized from methanol. The concentration of the stock solution of GdnHCl was calculated from refractive index measurements by the method of Nozaki (43). Protein solutions were incubated overnight at room temperature with different molarities of GdnHCl in 0.1 M phosphate buffer to ensure that equilibrium was attained before measurements were made. The wavelength of maximum emission of the

[1] The abbreviations used are: PAGE, polyacrylamide gel electrophoresis; HPLC, high performance liquid chromatography; GdnHCl, guanidine hydrochloride.

protein was monitored from excitation at 280 nm. The protein concentration was 0.1 mg/ml in each case. The temperature dependence of denaturation of the crystallins was monitored by change in the fluorescence emission maximum. On the basis of a two-state mechanism of unfolding, $N \rightleftharpoons D$, where N is the native state and D is the denatured state, the equilibrium constant of denaturation (K) was calculated by the method of Pace *et al.* (44, 45) using the expression $K = (\lambda_N - \lambda_O)/(\lambda_O - \lambda_D)$, where λ_N is the wavelength corresponding to maximum emission upon excitation at 280 nm for the native protein, λ_O is the emission maximum of the points in the transition region, and λ_D is that of the denatured protein. Using the van't Hoff plot of $-R \ln K$ *versus* $1/T$, the slope of the curve, *i.e.* enthalpy change (ΔH), can be determined. The midpoint of the transition corresponds to $T_{1/2}$. The entropy change can then be calculated from the equation $\Delta G = \Delta H - T\Delta S$ since ΔG is zero at the melting temperature $T_{1/2}$. The free energy of denaturation (ΔG_D) was estimated from the relationship $\Delta G_D = -RT \ln K$, where R is the gas constant (1.987 cal degree^{-1} mol^{-1}), T is the absolute temperature, and K was calculated as described above. For measuring the conformational stability in the absence of GdnHCl ($\Delta G_D(H_2O)$), it was assumed that the linear dependence of ΔG with denaturant concentration continues to zero concentration of GdnHCl (45). A least-squares analysis was then used to fit the data to the equation $\Delta G = \Delta G_D(H_2O) - m[\text{GdnHCl}]$, where m is a measure of the dependence of ΔG on denaturant concentration. The concentration of GdnHCl at the midpoint of the unfolding curve is given by $[\text{GdnHCl}]_{1/2} = \Delta G_D(H_2O)/m$.

RESULTS

We find that the extent of glycation that occurs in α-crystallin (nanomoles of fructose/nanomole of polypeptide) is about one-fifth of that which occurs in γ-crystallin upon incubation of the proteins with 0.5 M fructose for a period of a little over 2 months under identical conditions. About 2.4 nmol of formaldehyde are released from each nanomole of glycated α-crystallin through periodate oxidation of C-1 hydroxyls in the Amadori product form of the glycated protein (CH_2O/protein ratio of 2.4), as compared to 11.9 nmol of formaldehyde released from each nanomole of glycated γ-crystallin (CH_2O/protein ratio of 11.9). Swamy and Abraham (33) have shown that crystallin glycation saturates by 2 months *in vitro* under essentially similar conditions, while the process, in general, is much slower *in vivo*. A comparison of sequences shows that the potential sites for glycation (*i.e.* the basic residues Lys and Arg and a free NH_2 terminus) in the polypeptide chains of α- and γ-crystallins are similar in number. The various monomeric γ-crystallins have 2 lysines each, a free NH_2 terminus, and 20 arginine residues in a chain length of 174 amino acids. On the other hand, the 173-amino acid long αA and αB chains, which occur in a ratio of 3:1 in the 800-kDa α-particle, have 7 and 10 lysines each, blocked NH_2 termini, and 13 and 14 arginines, respectively. The poorer glycation of α-crystallin thus indicates that many basic residues in this protein do not react with fructose. This could arise from the buried state of some cationic residues in α-crystallin, as argued later.

A protein may be expected to become more acidic upon glycation since glycation leads to the neutralization of positive charges in the protein. Fig. 2*A* shows that the pI values of the various monomeric γ-crystallin chains are altered from the usual range of 7–8.5 to ~5–6. In this case, glycation also seems to reduce existing charge differences between the γ-crystallin chains; the glycated protein is localized on the isoelectric focusing gel almost as a single band. A similar acidification is seen in α-crystallin (Fig. 2*B*), which has a pI of 4.4–4.85. Glycated α-crystallin shows bands on the isoelectric focusing gel ranging from pI 3.1 to 4.6.

We detected the formation of covalent non-disulfide intermolecular cross-links in both γ- and α-crystallins in SDS-PAGE electrophoretic runs. Data for α-crystallin are presented in Fig. 3 (data for γ-crystallin is not shown).[2] Intermolecular cross-

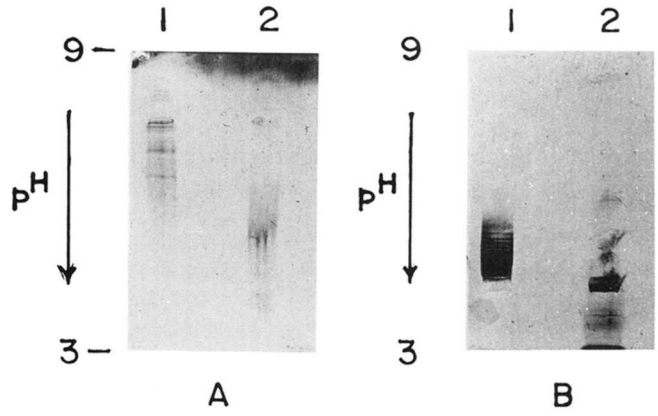

FIG. 2. **Isoelectric focusing profile at pH 3–9 of crystallins.** Samples of γ- and α-crystallins were incubated with 0.5 M fructose in 0.05 M phosphate buffer, pH 7.4, for a period of over 8 weeks under sterile conditions. *A*, *lane 1*, control; *lane 2*, glycated γ-crystallin. *B*, *lane 1*, control; *lane 2*, glycated α-crystallin. Bands were visualized by silver staining.

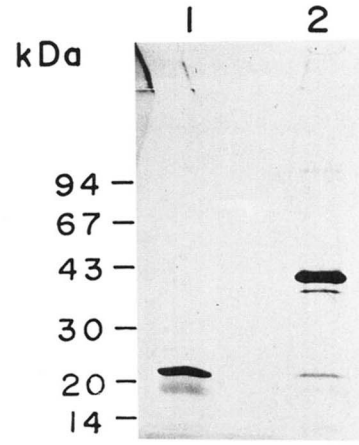

FIG. 3. **SDS-PAGE (12.5%) of α-crystallin incubated with fructose under same conditions as described for Fig. 2.** *Lanes 1* and *2*, control (0.15 mg/ml) and glycated (0.15 mg/ml) α-crystallin solutions, respectively. The gel was silver-stained for visualization of the protein bands.

linking of α-crystallin is found to have generated a population of dimers (constituting 90% fraction of the α-population) that is visualized on the gel in the form of two bands with molecular masses in the range of 40–42 kDa. These bands could have resulted from the homomeric or heteromeric cross-linking of αA and αB chains. Such cross-links have been observed earlier in lysozyme incubated with fructose 6-phosphate (29) and also in calf lens crystallins incubated with glucose 6-phosphate (47).

Both γ- and α-crystallins display increased absorption in the entire region from 220 to 600 nm upon glycation. Glycation also leads to a decreased fluorescence from tryptophan (Fig. 4, *A* and *B*) and an increase in the non-tryptophan fluorescence (*C* and *D*). These results are similar to those obtained upon the glycation of crystallins with glucose 6-phosphate (47). Synchronous fluorescence scanning (48) of solutions of the fructated γ- and α-crystallins (Fig. 4, *C* and *D*) indicates the presence of chromophores with excitation maxima at longer wavelengths; in the synchronous mode, the fructated protein displays excitation maxima at 335 and 385 nm (in addition to the 280 nm

[2] During staining of gels with alkaline ammoniacal silver nitrate, silver reacts with the positively charged groups on proteins (46). Since glycation results in the neutralization of positive charges, it may be expected to cause weakened silver staining of proteins. We found this to be particularly true of γ-crystallin, which was glycated to a greater extent than α-crystallin. Glycated γ-crystallin did not stain well with Coomassie Blue either.

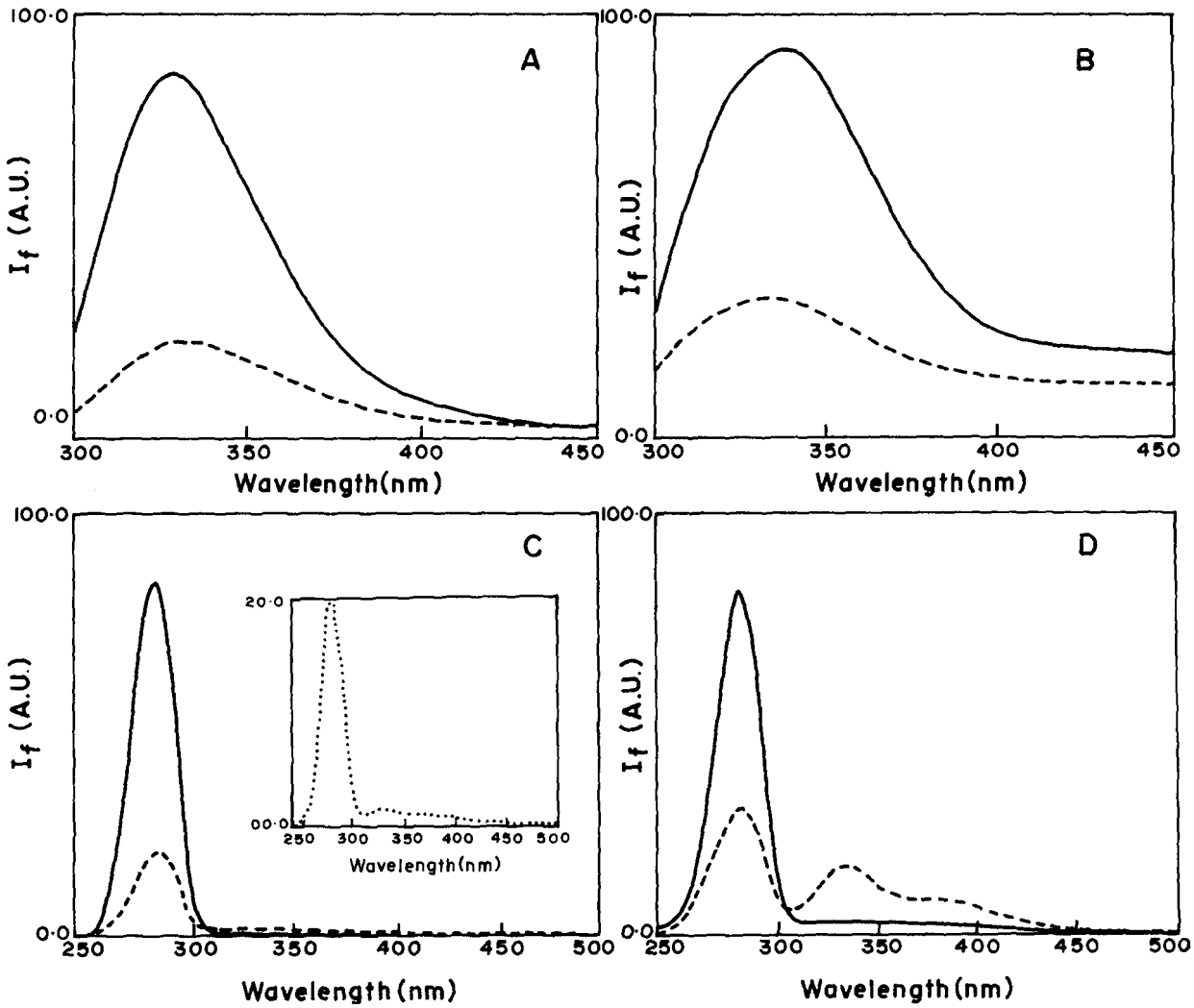

FIG. 4. **Tryptophan fluorescence spectra (excitation at 280 nm) of 0.1 mg/ml γ-crystallin (*A*) and α-crystallin (*B*) solutions incubated with (- - -) and without (——) 0.5 M fructose (control) and synchronous fluorescence scan (Δλ= 40 nm) of 0.1 mg/ml γ-crystallin (*C*) and α-crystallin (*D*) solutions incubated with (- - -) and without (——) 0.5 M fructose (control).** The *inset* in *C* shows the synchronous scan of glycated γ-crystallin on a different scale. Note the formation of non-tryptophan fluorophores with excitations at 335 and 385 nm in both glycated crystallins (*C* and *D*). I_f, intensity of fluorescence; *A.U.*, arbitrary units.

peak corresponding to the Tyr and Trp residues), which are absent in the unglycated protein.

Alterations in Secondary and Tertiary Structures

The fluorescence emission maximum in both crystallins was altered upon glycation. While the emission maximum of γ-crystallin (Fig. 4*A*) was found to have shifted toward the red (from 328 to 331 nm), that of α-crystallin (Fig. 4*B*) was found to have shifted toward the blue (from 335 to 332 nm). Thus, in γ-crystallin, fructation leads to an increased exposure of Trp residues to the solvent medium, while the opposite happens in α-crystallin.

Such contrasting results are also observed in the far-UV CD spectra of the normal and glycated proteins. The peptide chains of both γ- and α-crystallins are largely made up of the antiparallel β-pleated sheets (49), reflected by the presence of a negative CD band centered around 218 nm (Fig. 5, *A* and *B*). Glycation of γ-crystallin results in a reduction in the ellipticity value of this band (Fig. 5*A*), indicative of a reduction in secondary structural content.[3] In α-crystallin, on the other hand, there is an increase in secondary structural content upon fructation (Fig. 5*B*). The CD results suggest that while fructation tends to unfold γ-crystallin, it enhances the secondary structural order in α-crystallin.

The near-UV CD spectra in the region of 250–370 nm (Fig. 6, *A* and *B*), indicative of the disposition of aromatic residues in the proteins, also show substantial changes. In both modified crystallins, a new positive band is observed between 300 and 340 nm. The ^1L_b band of Trp near 300 nm, seen in the parent proteins, appears affected upon glycation. Also, the bands in the 280–260 nm region, due to Trp, Tyr, and Phe, are enhanced; this increased rotational strength suggests a greater loss of flexibility or increased electronic interactions, or both. These results are similar to those reported earlier by other workers (37–39).

Quaternary Structural Changes in Glycated α-Crystallin

The gel filtration behavior of control and fructated samples of α-crystallin was studied in the presence of different concentrations of GdnHCl using high performance liquid chromatography. In 50 mM phosphate buffer, pH 6.8, α-crystallin elutes from

[3] A. Pande, personal communication. Working with purified γ_{II}-crystallins, Pande has not observed any changes in the far-UV CD spectrum upon fructation. This would suggest that the other members of the γ-crystallin family are more vulnerable to fructation-mediated secondary structural change.

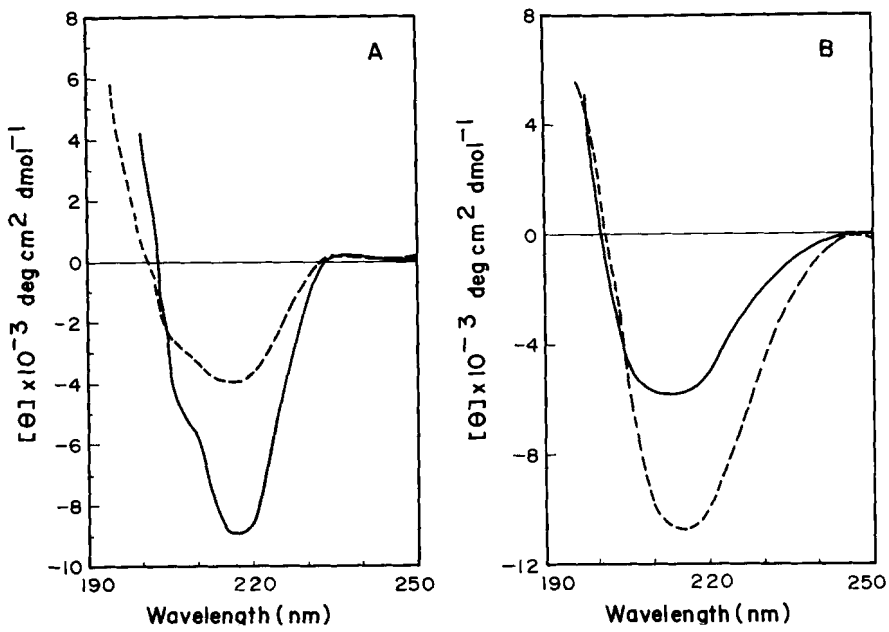

FIG. 5. **Circular dichroic spectra of control (——) and glycated (- - -) γ-crystallins (*A*) and control (——) and glycated (- - -) α-crystallins (*B*) in the far-UV region.**

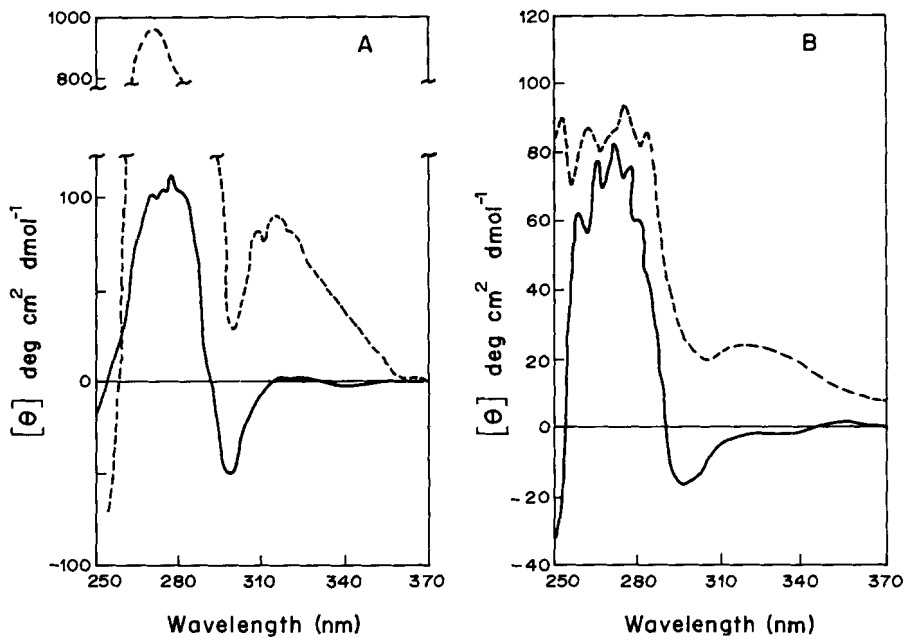

FIG. 6. **Circular dichroic spectra of control (——) and glycated (- - -) γ-crystallins (*A*) and control (——) and glycated (- - -) α-crystallins (*B*) in the near-UV region.**

a gel filtration column in two ranges of molecular mass. For the system of columns used in these experiments, one range consisting of two easily discernible components eluted close to the void volume, while another, also comprising two components, was found to elute close to the bed volume. Specifically, the two early components eluted at 40 min (peak 1) and 50 min (peak 2), respectively, in both control and fructated α-crystallins. These correspond to the 1100- and 800-kDa high molecular mass fractions of α-crystallin, respectively. The latter two components eluted at 95–98 min (peak 3) and 101–112 min (peak 4) for different concentrations of GdnHCl in control α-crystallin and similarly at 95–99 min (peak 3) and 101–104 min (peak 4) in the modified protein. It is not clear whether these represent only dimeric/monomeric αA and αB crystallins or whether smaller fragments of the protein, which are occasionally seen in the lens (50), are also represented. Calibration by standard gel filtration molecular mass markers showed that peak 3 corresponds to the dimeric (≈40–44-kDa) form, and peak 4 to the monomeric (or even the further fragmented) form of α-crystallin.

The elution profiles of the parent and glycated α-crystallin samples in phosphate buffer, pH 6.8, were found to be strikingly different, even for the native forms chromatographed in the absence of GdnHCl. Table I illustrates this point in some detail. While 70% of control α-crystallin eluted in peak 4 and only 24% eluted in peak 2, the elution pattern of glycated α-crystallin was 83% in peak 2, 8% in peak 3, and 5% in peak 4, indicating that glycation results in a preference for the higher molecular mass form of the protein.

In the presence of increasing concentrations of the denaturant, both the control and glycated forms of the protein were found to dissociate to smaller sizes. However, while control α-crystallin eventually dissociated to elute maximally at peak 4 (94%) at a GdnHCl concentration of 0.4 M, the modified protein eluted maximally at peak 3 (94%) under the same conditions. Thus, the glycated protein dissociated into a low molecular mass population comprising mostly dimers, while the control protein dissociated into a population of (mostly) monomers. (This is consistent with the SDS-PAGE results in Fig. 3, which show that a substantial fraction (90%) of the glycated α-crys-

tallin consists of covalently cross-linked dimers.) The percentage of control α-crystallin eluting at peak 2 dropped from 20% at 0.1 M GdnHCl to 4% at 0.2 M GdnHCl. A sharper transition was observed for the glycated protein between 0.2 and 0.25 M GdnHCl, as is evident from Table I. At a concentration of 0.25 M GdnHCl, the elutions corresponding to peaks 1 and 2 disappear in both cases, and only those corresponding to peaks 3 and 4 remain.

The quaternary structure of α-crystallin is known to be sensitive to pH and ionic strength (51). Thus, at pH 6.8 (with no denaturant in solution), only 24% of control α-crystallin exists in the form of the 800-kDa particle, whereas at pH 7.5, essentially all of α-crystallin exists in the form of the 800-kDa particle. The above HPLC runs at pH 6.8 therefore suggest that the glycated form of α-crystallin displays an increased resistance to pH-induced as well as GdnHCl-induced dissociation of subunits.

The fluorescence emission maximum of either the glycated or unmodified form of the protein is not seen to alter in the range of GdnHCl concentrations (0–0.25 M) used above (data not shown). Thus, dissociation of α-crystallin subunits does not seem to involve any unfolding of the individual subunits in this range of denaturant concentration.

TABLE I
Effect of GdnHCl on HPLC gel filtration profiles of control and glycated α-crystallins
Peaks 1–4 eluted at 40, 50, 95–98, and 101–112 min, respectively.

GdnHCl	Distribution in HPLC peaks			
	Peak 1	Peak 2	Peak 3	Peak 4
			%	
0.0 M				
Control	6	24	1	70
Glycated	4	83	8	5
0.1 M				
Control	2	20	5	74
Glycated	2	90	9	
0.2 M				
Control	1	4	4	92
Glycated	5	44	51	
0.25 M				
Control	1		10	90
Glycated			80	21
0.4 M				
Control			6	94
Glycated			94	6

Stability of Native Structure

Denaturation with Guanidine Hydrochloride—Fig. 7 shows the denaturation behavior of the unmodified and glycated forms of γ- and α-crystallins with increasing concentrations of GdnHCl. The parameters calculated from the chemical denaturation curves of these proteins are listed in Table II. The free energy of GdnHCl denaturation ($\Delta G_D(H_2O)$) of the control γ-crystallin at room temperature (~27 °C) was estimated to be 3.81 kcal/mol. This value is lower than the values reported for γ-crystallins by Kono *et al.* (52), probably reflecting the differences in solution conditions; however, the *m* values in the two studies are the same. In comparison, glycated γ-crystallin denatures at a lower GdnHCl concentration and with a lower $\Delta G_D(H_2O)$ value (2.0 *versus* 3.0 M GdnHCl and 1.8 *versus* 3.8 kcal/mol). This is consistent with our spectral results above, which suggest that glycation tends to reduce the secondary structural order in γ-crystallin.

In contrast, glycated α-crystallin needs a higher GdnHCl concentration than the unmodified protein to denature (1.8 *versus* 1.3 M GdnHCl). The free energy of GdnHCl denaturation is marginally higher than that of the parent α-crystallin (1.4 *versus* 1.1 kcal/mol). This is again consistent with our spectral results on α-crystallin, which show the glycated molecule to have a higher degree of secondary structural order.

Thermal Denaturation—Fig. 8*A* shows the thermal unfolding curves of control and modified γ-crystallins. The glycated molecule is seen to denature at a lower temperature (T_m = 62 °C) than the control protein (72 °C). The sharpness of the thermal melting profile is comparable in both cases. We have used these data to estimate the denaturation enthalpy and entropy, assuming a two-state model for the process. The thermodynamic parameters calculated for the γ-crystallins using the van't Hoff plot (Fig. 8*B*) are given in Table III. Besides the lowered melting temperature, glycated γ-crystallin also has reduced values of ΔH and ΔS of denaturation. Upon complete

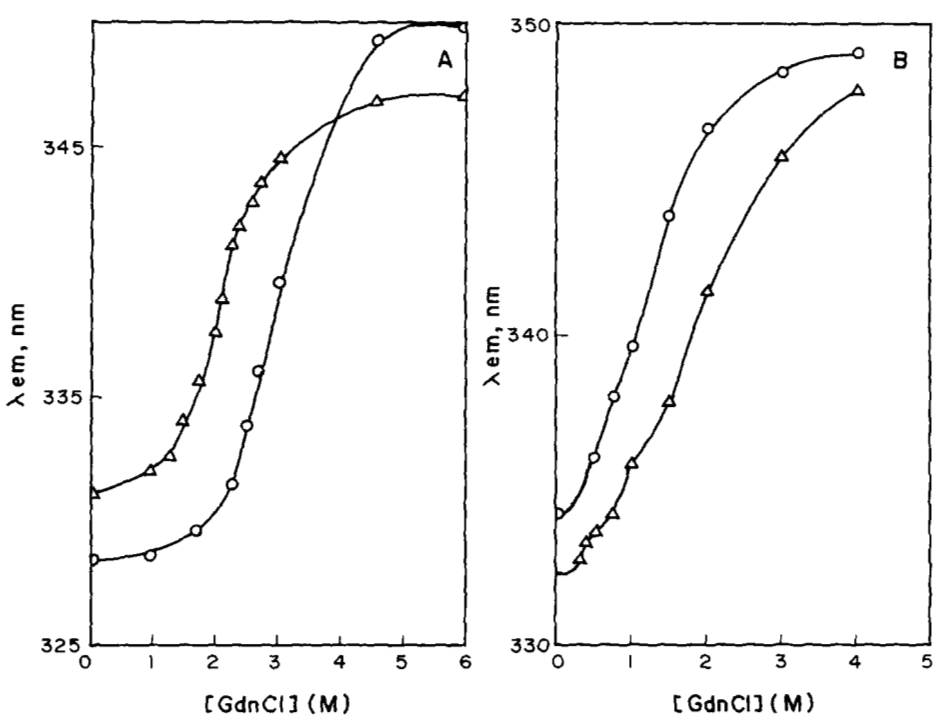

FIG. 7. **Denaturation profile of control (○) and glycated (△) γ-crystallins (*A*) and α-crystallins (*B*) in presence of GdnHCl as monitored by changes in fluorescence emission maximum.**

unfolding at 85 °C, the fluorescence emission maximum shifts from 328 to 342 nm in the control protein, whereas it moves from 331 to 345 nm in the glycated protein.

The situation with α-crystallin is somewhat different. While a single-phase rise in the emission band maximum of control α-crystallin is observed, glycated α-crystallin shows a biphasic transition with temperature, as shown in Fig. 9.

DISCUSSION

Since the energetic cost of placing an electrically charged residue in a low dielectric or apolar medium is significant (53), the side chains of charged residues tend to occur on the surface of a globular protein (54, 55). Even here, oppositely charged residues tend to come together, to the extent that the sequence and secondary structure permit, to form ion pairs that contribute to protein stability (56). Thus, one sees that many globular proteins tend to have optimum stability when their net charge is minimized, *i.e.* at the isoelectric point (57). Any alteration in the charge pattern of the protein, brought about by a change in the medium's pH or by chemical modification of the charged residues, would be expected to alter the stability of the native structure of the protein.

Since the pH at which these measurements were made (pH 6.8) corresponds to the physiological pH of the lens (≈pH 7.0), a net destabilizing charge exists in the crystallins at this pH to begin with. γ-Crystallin is positively charged, while α-crystallin is negatively charged. Since glycation leads to the neutralization of positive charges, it would be expected to stabilize the basic γ-crystallin by reducing repulsive interactions between positive charges on the protein's surface. However, the situation would be different if the neutralization of positive charges were to reverse the balance of charges and convert the basic protein to an acidic protein (pI <7.0). We find that such a reversal occurs upon glycation of γ-crystallin. The pI values of γ-crystallin molecules range from 7.0 to 8.5. Upon glycation, this value is shifted to a range of 5.0–6.0. The net negative charge on the protein at pH 7.0 now exceeds the net positive charge that existed on the protein prior to glycation. Thus, the increased repulsive interactions in the glycated form of γ-crystallin tend to destabilize it.

γ-Crystallin is a kidney-shaped molecule, with the NH_2-terminal domain comprising 14 positive and 13 negatively charged residues and the COOH-terminal domain comprising eight positive and seven negative charges. Lindley *et al.* have shown (58) that an extensive network of ion pair-forming residues is located on the molecule's surface. The state of charge on these residues affects the conformational stability of the protein; alteration of the charge profile of γ-crystallin, through changing of solution pH to alkaline (pH ≈11.0) (59) or acidic values (pH ≈3.0), tends to denature it. Glycation could affect conformational stability adversely through the disruption of "stabilizing" ion pairs. Also, the neutralization of positive charges in closely spaced ion pairs could be expected to result in increased coulombic repulsions between negatively charged residues.

The case of the cortical protein α-crystallin is different in several ways from that of the nuclear protein γ-crystallin. In γ-crystallin, the experimentally determined pI values agree with the theoretically calculated values (using the p*K* values of the constituent Lys, Arg, His, Asp, and Glu residues in the sequence), showing that no charges are "buried" in the apolar interior of the globular protein. It seems, however, that α-crystallin contains buried basic residues. First, the experimentally determined pI range of α-crystallin (4.4–4.8) is lower than the computed pI values of the α-crystallin chains (αA (5.52) and αB (6.86)) (see "Materials and Methods"). This suggests that some cationic residues are buried within the interior of the protein. Second, α-crystallin is a highly aggregated protein, with a dynamic quaternary structure that is comparable to those of surfactant micelles (36). This would explain the observation (see above) that glycation of α-crystallin does not occur to the extent

TABLE II
Free energy of GdnHCl denaturation in water of unmodified and glycated crystallins

Protein	$\Delta G_D(H_2O)$	*m*	$[GdnHCl]_{½}$
	kcal mol^{-1}	(*kcal mol*$^{-1}$ *M*$^{-1}$)	*M*
Control γ	3.8	−1.3	3.0
Glycated γ	1.8	−0.9	2.0
Control α	1.1	−0.9	1.3
Glycated α	1.4	−0.8	1.8

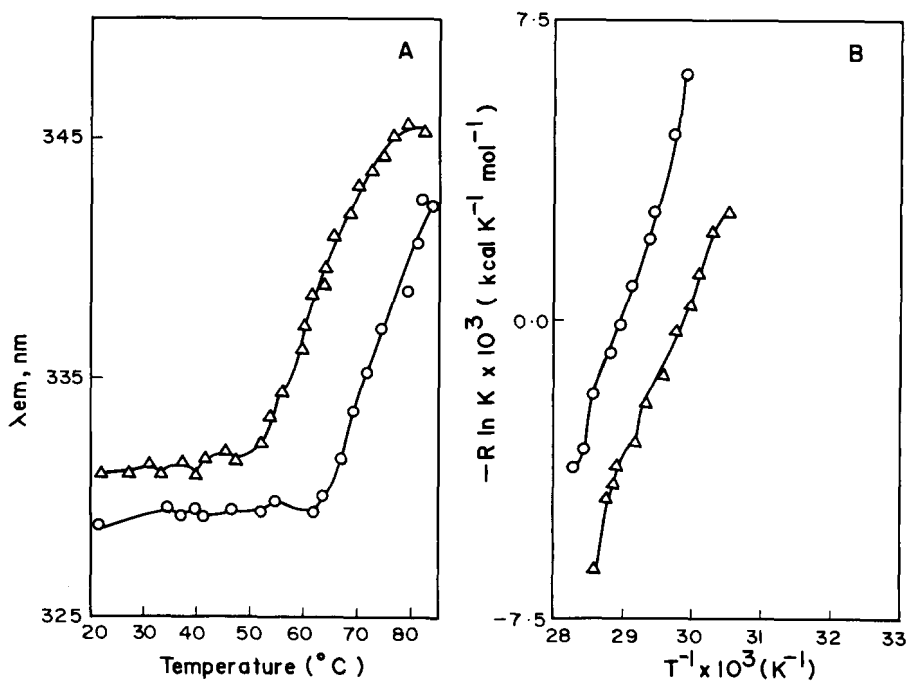

FIG. 8. *A*, plot of the variation of the wavelength of maximum emission (upon excitation at 280 nm) *versus* temperature; *B*, van't Hoff plot of the denaturation with increase in temperature of control (○) and glycated (△) γ-crystallins.

TABLE III
Thermodynamic parameters derived from thermal denaturation of unmodified and glycated γ-crystallins

Protein	$T_{1/2}$	ΔH	ΔS
	°C	kcal mol^{-1}	kcal mol^{-1} K^{-1}
Control protein	72	52.5	152
Glycated protein	62	44.5	132

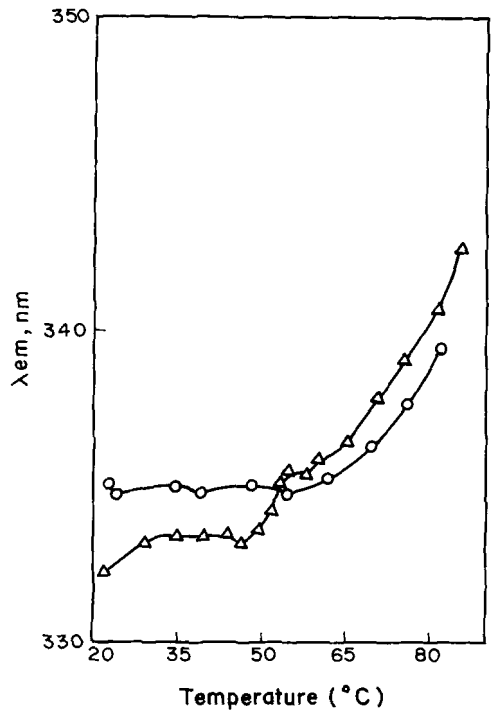

FIG. 9. **Temperature dependence of fluorescence emission maximum (upon excitation at 280 nm) of 0.1 mg/ml solutions of control (○) and glycated ( ) α-crystallins in 0.1 M phosphate buffer, pH 7.0.**

expected from its sequence and is lower than that of γ-crystallin.

Stigter and Dill (60) have pointed out that the pH of maximum stability of a protein that contains buried charges is not the same as its pI. Augusteyn *et al.* (51) have shown that the pH of optimum stability of α-crystallin is around pH 7–8, well above its pI. These authors have also shown that the molecule starts to denature at a pH of 4.5. Thus, α-crystallin would appear to be more stable at neutral pH than at its pI. This indicates that the progressive neutralization of the $-NH_3^+$ groups with the increase in pH may be expected to increase the conformational stability of the protein. Such a neutralization of positive groups occurs upon glycation, which appears to be the reason why glycated α-crystallin has a higher secondary as well as quaternary structural order.

There are some features of the thermal denaturation of the modified and unmodified forms of α-crystallin that are worthy of comment. While chemical denaturation (Fig. 7*B*) shows that glycated α-crystallin undergoes a single-phase transition, the thermal denaturation profile shows multiple transitions.

The thermal denaturation profile of α-crystallin monitored by spectroscopy and differential scanning calorimetry has revealed (36, 61) that the protein is assembled as a 42-mer aggregate (molecular mass of 800 kDa), which dissociates into a loosely held aggregate around 45 °C and further into a 18-mer particle (360 kDa) beyond 60 °C. This 360-kDa particle is heat-stable even up to 100 °C. The first transition appears to be seen only in differential scanning calorimetry and is concentration-dependent; it is not seen in conventional spectral assays (36). In accordance with these observations, we also find a single-phase rise in the emission band maximum of control α-crystallin with temperature (Fig. 9, ○). In contrast, however, the thermal denaturation profile of glycated α-crystallin as shown in Fig. 9 involves two steps. At temperatures below 45 °C, the emission band occurs near 332 nm, which, being lower than that in the unglycated protein, suggests that the Trp residues face a more apolar environment than in the control protein. The first transition occurs upon heating to ~50 °C, when the emission maximum red-shifts to ~335–336 nm, and further heating beyond 60 °C leads to a monotonic increase in the emission wavelength just as it occurs with the unglycated protein.

The fact that glycation increases the chain order of α-crystallin and makes the Trp environment somewhat more apolar suggests that the glycated protein might adopt the 42-mer structure with greater facility than the free protein. The transition seen at ~50 °C would then yield the loosely held oligomeric structure, which rearranges beyond 60 °C to a population of the 18-mer 360-kDa particle. This proposition is borne out by the observation made by Walsh *et al.* (36) that the subunits of the third layer in the 800-kDa particle are loosely bound by both polar and apolar forces. Glycation would cause a reduction in the ionic interactions between subunits, which could influence the nature of their associative behavior at high temperatures.

Fructation-induced changes in the color, structure, and stability of the crystallins are relevant to the molecular changes that might occur in the diabetic eye lens and its compromised function. The accumulation of colored compounds should affect the broad-band wavelength transmission characteristics of the lens. The tendency of γ-crystallin to unfold upon glycation could result in altered intermolecular packing, and the acidification of the glycated molecule might affect its solubility. Fructation appears to induce a greater tendency for aggregation in the cortical α-crystallin, which could increase the scattering of light by such modified material. Increased light scattering will also be displayed by the intermolecularly cross-linked protein aggregates that are generated by the fructation reaction.

Acknowledgments—We are thankful to Purnananda Guptasarma for valuable discussions and for help with the preparation of this manuscript. We thank Ch. Mohan Rao and Dipankar Chatterjee for comments on the manuscript.

REFERENCES

1. Baynes, J. W., Watkins, N. G., Fisher, C. I., Hull, C. J., Patrick, J. S., Ahmed, M. U., Dunn, J. A., and Thorpe, S. R. (1989) in *The Maillard Reaction in Aging, Diabetes, and Nutrition* (Baynes, J. W., and Monnier, V. M., eds) pp. 43–67, Alan R. Liss, Inc., New York
2. Krantz, S., Lober, M., and Henschel, L. (1986) *Exp. Clin. Endocrinol.* **88,** 257–269
3. Njoroge, F. G., and Monnier, V. M. (1989) in *The Maillard Reaction in Aging, Diabetes, and Nutrition* (Baynes, J. W., and Monnier, V. M., eds) pp. 85–107, Alan R. Liss, Inc., New York
4. Hayase, F., Nagaraj, R. H., Miyata, S., Njoroge, F. G., and Monnier, V. M. (1989) *J. Biol. Chem.* **264,** 3758–3764
5. McPherson, J. D., Shilton, B., and Walton, D. J. (1988) *Biochemistry* **27,** 1901–1907
6. Suarez, G., Rajaram, R., Oronsky, A. L., and Gawinowicz, M. A. (1989) *J. Biol. Chem.* **264,** 3674–3679
7. Lee, H. S., Sen, L. C., Clifford, A. J., Whitaker, J. R., and Feeney, R. E. (1979) *J. Agric. Food Sci.* **27,** 1094–1098
8. Bunn, H. F., and Higgins, P. J. (1981) *Science* **213,** 222–224
9. Horiuchi, S., Araki, N., and Morino, Y. (1991) *J. Biol. Chem.* **266,** 7329–7332
10. Araki, N., Ueno, N., Chakrabarti, B., Morino, Y., and Horiuchi, S. (1992) *J. Biol. Chem.* **267,** 10211–10214
11. Makita, Z., Vlassara, H., Cerami, A., and Bucala, R. (1992) *J. Biol. Chem.* **267,** 5133–5138
12. Kohn, R. R., and Monnier, V. M. (1987) in *Clinical Pharmacology in the Elderly* (Swift, C. G., ed) pp. 3–30, Marcel Dekker, Inc., New York
13. Cerami, A., Vlassara, H., and Brownlee, M. (1986) *J. Cell. Biochem.* **30,** 111–120
14. Vlassara, H., Valinsky, J., Brownlee, M., Cerami, C., Nishimoto, S., and Cerami, A. (1987) *J. Exp. Med.* **166,** 539–549

15. Monnier, V. M., Stevens, V. J., and Cerami, A. (1979) *J. Exp. Med.* **150,** 1098–1107
16. Hamlin, C. R., Kohn, R. R., and Luschin, J. H. (1975) *Diabetes* **24,** 902–904
17. Elbe, A. S., Thorpe, S. R., and Baynes, J. W. (1983) *J. Biol. Chem.* **258,** 9406–9412
18. Pongor, S., Ulrich, P. C., Bencsath, F. A., and Cerami, A. (1984) *Proc. Natl. Acad. Sci. U. S. A.* **81,** 2684–2688
19. Schnider, S. L., and Kohn, R. R. (1981) *J. Clin. Invest.* **67,** 1630–1635
20. Monnier, V. M., Sell, D. R., Abdul-Karim, F., and Emancipator, S. (1988) *Diabetes* **37,** 867–872
21. Brownlee, M., Vlassara, H., Kooney, A., Ulrich, P., and Cerami, A. (1986) *Science* **232,** 1629–1632
22. Luthra, M., Sundari, C. S., Guptasarma, P., and Balasubramanian, D. (1991) in *Molecular Conformations and Biological Interactions* (Balaram, P., and Ramaseshan, S., eds) pp. 281–293, Indian Academy of Sciences, Bangalore, India
23. Sharma, Y., Rao, C. M., Narasu, M. L., Rao, S. C., Somasundaram, T., Gopalakrishna, A., and Balasubramanian, D. (1989) *J. Biol. Chem.* **264,** 12794–12799
24. Guptasarma, P., Balasubramanian, D., Matsugo, S., and Saito, I. (1992) *Biochemistry* **31,** 4296–4303
25. Hoenders, H. J., and Bloemendal, H. (1981) in *Molecular and Cellular Biology of the Eye Lens* (Bloemendal, H., ed) pp. 279–326, John Wiley & Sons, New York
26. Delaye, M., and Tardieu, A. (1983) *Nature* **302,** 415–417
27. Benedek, G. B. (1971) *Appl. Optics* **10,** 459–473
28. Bettelheim, F. A., and Siew, E. L. (1983) *Biophys. J.* **41,** 29–33
29. Szwergold, B. S., Kappler, F., and Brown, T. R. (1990) *Science* **247,** 451–454
30. Stevens, V. J., Rouzer, C. A., Monnier, V. M., and Cerami, A. (1978) *Proc. Natl. Acad. Sci. U. S. A.* **75,** 2918–2922
31. Swamy, M. S., Perry, R. E., and Abraham, E. C. (1987) *Fed. Proc.* **46,** 2153
32. Liang, J. N., and Chylack, L. T. (1987) *Invest. Ophthalmol. & Visual Sci.* **28,** 790–794
33. Swamy, M. S., and Abraham, E. C. (1991) *Exp. Eye Res.* **52,** 439–444
34. Abraham, E. C., Swamy, M. S., and Perry, R. E. (1989) in *The Maillard Reaction in Aging, Diabetes, and Nutrition* (Baynes, J. W., and Monnier, V. M., Eds) pp. 123–139, Alan R. Liss, Inc., New York
35. Gabbay, K. H., and Kinoshita, J. H. S. (1972) *Isr. J. Med. Sci.* **8,** 1557–1561
36. Walsh, M. T., Sen, A. C., and Chakrabarti, B. (1991) *J. Biol. Chem.* **266,** 20079–20084
37. Liang, J., and Chakrabarti, B. (1981) *Biochem. Biophys. Res. Commun.* **102,** 180–189
38. Liang, J., and Chylack, L. T., Jr. (1984) *Biochem. Biophys. Res. Commun.* **123,** 899–906
39. Liang, J., and Ross, M. T.(1990) *Exp. Eye Res.* **50,** 367–371
40. Perry, R. E., Swamy, M. S., and Abraham, E. C. (1987) *Exp. Eye Res.* **44,** 269–289
41. Gallop, P. M., Fluckiger, R., Hannenken, A., Mininsohn, M. M., and Gabbay, K. H. (1981) *Anal. Biochem.* **117,** 427–432
42. Ahmed, N., and Furth, A. J. (1991) *Anal. Biochem.* **192,** 109–111
43. Nozaki, Y. (1972) *Methods Enzymol.* **26,** 43–50
44. Pace, C. N. (1975) *CRC Crit. Rev. Biochem.* **3,** 1–43
45. Pace, C. N., Shirley, B. A., and Thomson, J. A. (1989) in *Protein Structure: Practical Approach* (Creighton, T. E., ed) pp. 311–330, IRL Press, Oxford
46. Wray, W., Boulikas, T., Wray, V. P., and Hancock, R. (1981) *Anal. Biochem.* **118,** 197–203
47. van Boekel, M. A. M., and Hoenders, H. J. (1991) *Exp. Eye Res.* **53,** 89–94
48. Rao, C. M. (1991) *Biochem. Biophys. Res. Commun.* **176,** 1351–1357
49. Mandal, K., Bose, S. K., Chakrabarti, B., and Siezen, R. J. (1985) *Biochim. Biophys. Acta* **832,** 156–164
50. Russo, G., Vincenti, D., Ragone, R., Stiuso, P., and Colonna, G. (1992) *Biochemistry* **31,** 9279–9287
51. Augusteyn, R. C., Ellerton, H. D., Putilina, T., and Stevens, A. (1988) *Biochim. Biophys. Acta* **957** 192–201
52. Kono, M., Sen, A. C., and Chakrabarti, B. (1990) *Biochemistry* **29,** 464–470
53. Honig, B., Hubbel, W., and Flewelling, R. F. (1986) *Annu. Rev. Biophys. Biophys. Chem.* **15,** 163–193
54. Barlow, D. J., and Thornton, J. M. (1983) *J. Mol. Biol.* **168,** 867–885
55. Wada, A., and Nakamura, H. (1981) *Nature* **293,** 757–758
56. Fersht, A. R. (1972) *J. Mol. Biol.* **64,** 497–509
57. Pace, C. N. (1990) *Trends Biochem. Sci.* **15,** 14–17
58. Lindley, P. F., Narebor, M. E., Summers, L. J., and Wistow, G. J. (1985) in *The Ocular Lens: Structure, Function and Pathology* (Maisel, H., ed) pp. 123–167, Marcel Dekker, Inc., New York
59. Mandal, K., Chakrabarti, B., Thomson, J., and Siezen, R. J. (1987) *J. Biol. Chem.* **262,** 8096–8102
60. Stigter, D., and Dill, K. A. (1990) *Biochemistry* **29,** 1262–1271
61. Maiti, M., Kono, M., and Chakrabarti, B. (1988) *FEBS Lett.* **236,** 109–114 Excitation wavelength was 280 nm.